FATIGUE BEHAVIOR OF THROUGH THE THICKNESS REINFORCED JOINTS

S. Stelzer[a*], S. Ucsnik[b], H. Sehrschön[c], J. Tauchner[d], G. Pinter[a]

[a] *Montanuniversität Leoben, 8700 Leoben, Otto Glöckel-Straße 2, AUSTRIA*
[b] *LKR Leichtmetallkompetenzzentrum Ranshofen GmbH, Austrian Instiute of Technology, 5282 Ranshofen, Lamprechtshausenerstraße Postfach 26, AUSTRIA*
[c] *FILL GmbH, 4942 Gurten, Fillstraße 1, AUSTRIA*
[d] *FACC AG, 4910 Ried im Innkreis, Fischerstraße 9, AUSTRIA*

** steffen.stelzer@unileoben.ac.at*

Keywords: CFRP, fatigue, joining

Abstract
Fatigue measurements on Single Lap Shear specimens made of carbon fiber reinforced polymer were carried out. The interfaces of the specimens were reinforced with metallic pins in the through thickness direction. Besides classical S-N curves, stiffness based analysis methods were used to better understand the failure behavior of the joints in the progress of their fatigue life. Furthermore full field strain analysis gave information about damage initiation and growth in the joint section.

1. Introduction and background

Carbon fiber reinforced polymer (CFRP) composites are becoming increasingly important for structural applications in the transportation industry and other areas, where lightweight design is advantageous for operational costs. Along with this growing interest in designs based on CFRP comes the demand for through the thickness reinforcements and for joining technologies that account for the anisotropy and laminate structure of this material. Many researchers have faced the questions that arise with joining and the reinforcement of laminates in the through thickness direction [1–11]. Research groups around Cartié, Partridge, Aymerich or Mouritz carried out extensive research on stitched and z-fiber reinforced composites [12–15]. Ji, Son, Löbel, Cartié or Graham lead recent studies on the through thickness reinforcement with metal rods [4, 5, 7, 10, 11]. Some of these research works focused on static testing [1, 3, 6–11], some also dealt with the determination of the fatigue properties of these reinforcement technologies [1–5, 16–20]. In the present study a new bonding technology is presented. This joining technology aims at combining both joining mechanisms, form-fit and adhesive bonding, with an integrative joint approach. Arrays of vertical elevations (pins) are disposed on thin metal sheets. The formation of pins and pin arrays is realized by a cold metal transfer welding process (CMT) [21, 22]. The pins, see Figure 1 (a) are small in comparison to the overall specimen dimensions, they have a height of approximately 3 mm and possess a head which provides an undercut face. When dry or pre-impregnated fiber-textiles are placed onto the arrays of pins, the pins penetrate the single layers. They push aside the fibers and form a through the thickness reinforcement without damaging the fibers. In previous studies the monotonic failure behavior of metal pin

reinforced Single Lap Shear (SLS) CFRP to CFRP joints was investigated [23]. It was shown, that the damage tolerance of CFRP to CFRP joints can be increased significantly by using this technology.

The present study aims at the investigation of such novel joint SLS CFRP-CFRP specimens and the mechanical characterization under fatigue loads.

2. Experiments

2.1. Materials and specimens

The joint section of the specimens was reinforced with different versions of metal through the thickness reinforcements. The single SLS specimens were cut out of CFRP panels. Each CFRP panel consisted of biaxial non-crimp fabrics with a quasi-isotropic stacking sequence made of high tenacity, standard modulus fibers and RTM6 epoxy matrix. Detailed explanations of specimen shape, specimen reinforcement and manufacture methods are given in [23]. The metallic reinforcements used in these investigations consisted of thin metal sheets that carried arrays of pins with spiked-spherical endings on both sides (see Figure 1). The pins were welded via the CMT welding process given in [23]. The herein tested SLS-specimens were reinforced with inserts made of two different metal alloys: stainless steel and titanium. The stainless steel reinforcements consisted of 0.6 mm thin steel sheets of type AISI 304 and pins of type AISI 316L welded onto both sides of the metal sheet. In case of titanium, the metal sheets were a grade 5 Ti6Al4V alloy with a thickness of 0.4 mm and the pins were made of Ti6Al4V. In both cases of metal inserts 24 Pins were positioned on each side of the metallic sheet with 2 x 6 pins at each end of the joint section of the specimen.

2.2. Test methods

Fatigue tests were carried out on a servo-hydraulic test machine, type MTS 322, with a 250 kN load range. The frequency of the fatigue tests was fixed to 10 Hz in order to prevent hysteretic heating in the CFRP laps. The stress ratio R accounted to 0.1 for all tests. The tests were run until failure of the SLS specimens occurred or until a maximum number of cycles, $N=10^6$, was reached. Digital image correlation was used to get information about local strains and displacements on the specimen's surface. Furthermore, it was used to get information about damage initiation and growth in the joint section of the SLS specimens. Local hysteresis data was gathered at every n^{th} cycle.

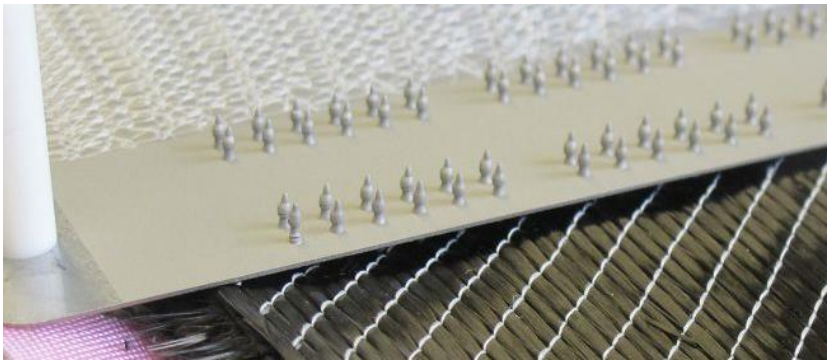

Figure 1. Draping of fibers on top of CMT welded stainless steel pin arrays.

For the stress-strain analysis engineering shear stresses, τ, were calculated via Equation (1) and local shear strains, $\tan\theta$, via Equation (2).

$$\tau = \frac{F}{A} \tag{1}$$

$$\tan\theta = \frac{\Delta l}{h} \tag{2}$$

In Equations (1) and (2) F represents the applied axial load, A the interface joint area, Δl the increase in distance between two points in loading direction and h the distance between two points in the thickness direction (z-direction) of the specimen. One reference point was placed on each CFRP lap in the middle of the joint area.

3. Results and discussion

Figure 2 shows the S-N curves for both the stainless steel pin reinforced (red lines) and the titanium pin reinforced SLS specimens (black lines). The S-N curve of the stainless steel pin reinforced samples reaches a higher level of stress, e.g. τ_{max}=4.6 MPa at 10^6 cycles ($\tau_{max,10^6}$), than the S-N curve of the titanium pin reinforced samples, $\tau_{max,10^6}$=3.4 MPa. Furthermore, there is an increase in the amount of scatter, quantified by $1/T_N$, from stainless steel pin reinforced to titanium pin reinforced samples. The range of scatter in number of cycles, T_N, gives the ratio of 10% probability of survival, P_{10}, to 90% probability of survival, P_{90}. The differences in the $\tau_{max,10^6}$ and $1/T_N$ values can be primarily ascribed to the lack of a pronounced spherical ending in the case of the titanium pins and the resulting weak form-fit with the surrounding CFRP.

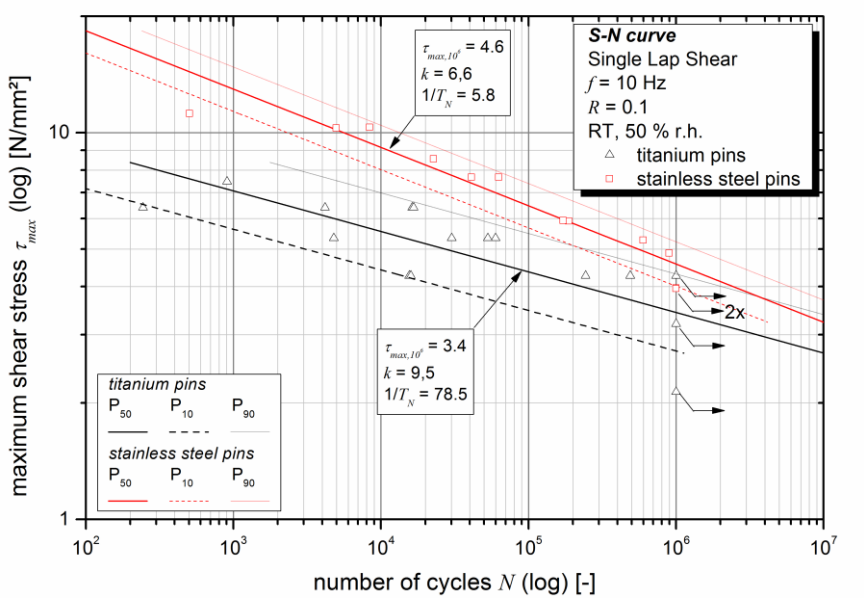

Figure 2. S-N curve for SLS specimens reinforced with CMT welded stainless steel (red lines) and titanium pins (black lines). P_{10}, P_{50} and P_{90} represent curves for 10, 50 and 90 % propability of survival, respectively. k is the exponent of the S-N curve and $1/T_N$ represents the scatter of the S-N curves between P_{10} and P_{90}.

The following post-processing and evaluation of hysteresis curves of the joints at different numbers of cycles (Figure 3) shows time dependent joining or material behavior. Increasing local shear strains at constant joint stiffnesses (slopes of the hysteresis curves), may imply visco-elastic material behavior, e.g. creep, which leads to a horizontal shift of the hysteresis curves. But this increase in local shear strain may also be due to damage initiation and growth of these damages in the joint section of the SLS specimen.

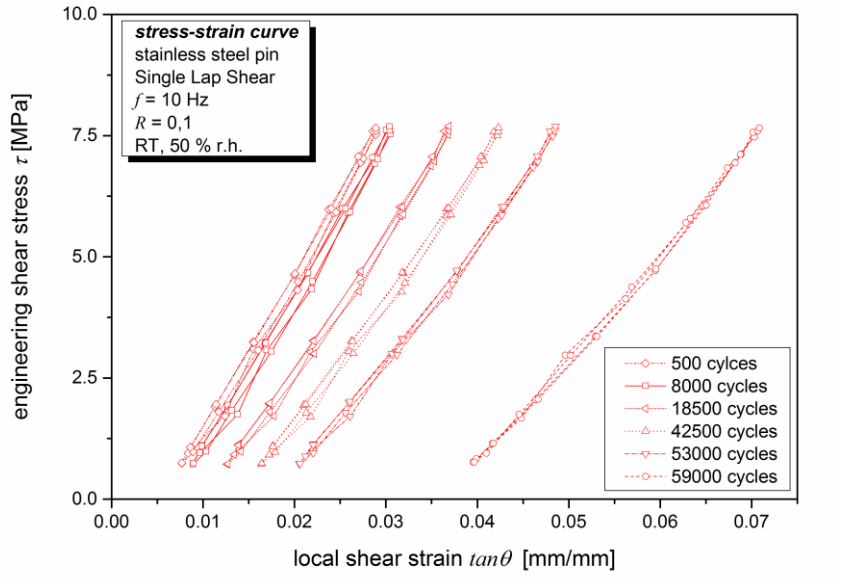

Figure 3. Stress-strain curves for a SLS specimen reinforced with CMT welded stainless steel pins. Failure occurred after 62747 cycles.

For the clarification of these effects, digital image correlation was used to get information on local deformation processes on the lateral surface of the specimen at different test stages. Pictures of the joint section at the respective number of cycles are shown in Table 1. The strain overlays show, that at the very beginning of the test the interface region is the most stressed region. Major strain concentrations occur at the ends of the connecting interface. In a progressed stage of the fatigue tests, in this case after about one third of the fatigue life of the specimen (N=18500), cracks occur in the interface region and subsequently the adhesive bonding fails. Nevertheless, the specimen is still able to carry loads until a maximum of ~ 63000 cycles, due to the remaining load carrying capability of the reinforcing pins.

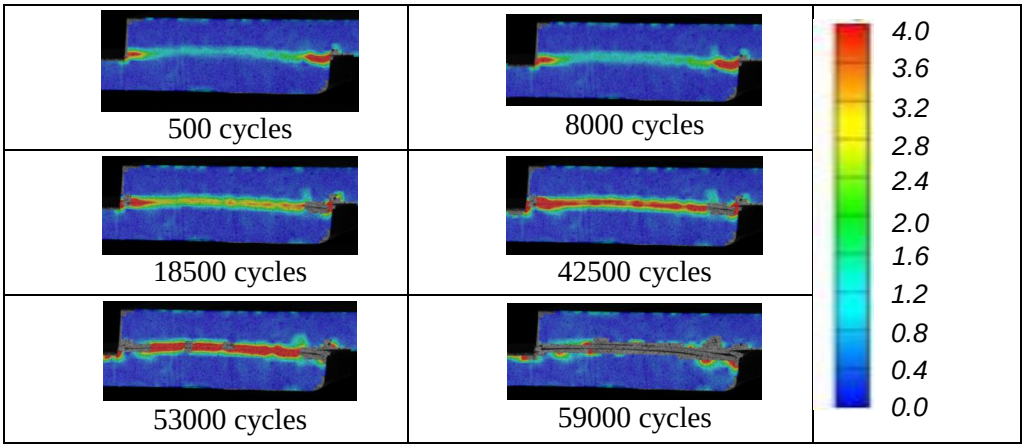

Table 1. Photographs of the lateral surface of a stainless steel pin reinforced specimen at different stages. The strain overlays from digital image correlation show the corresponding distributions of major strains.

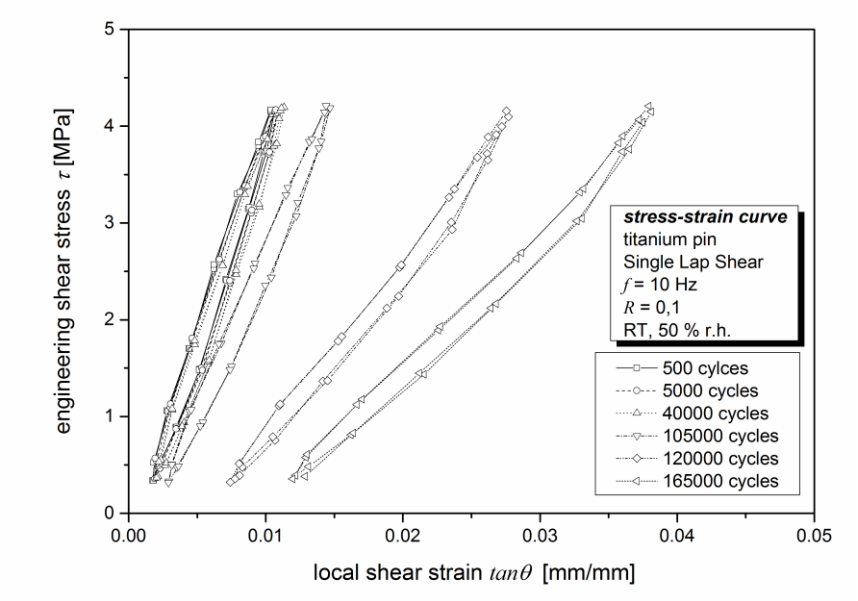

Figure 4. Stress-strain curves for a SLS specimen reinforced with CMT welded titanium pins. Failure occurred after 243319 cycles.

500 cycles	40000 cycles	4.0 3.6 3.2 2.8 2.4 2.0 1.6 1.2 0.8 0.4 0.0
105000 cycles	120000 cycles	
165000 cycles		

Table 2. Photographs of the lateral surface of a titanium pin reinforced specimen at different stages. The strain overlays from digital image correlation show the corresponding distributions of major strain.

The comparison of the failure behavior of the stainless steel pin reinforced SLS specimens and titanium pin reinforced specimens shows that titanium pin reinforced joints underwent significant losses in joint stiffness. This is due to the failure of the adhesive bond line between the metal sheet carrying the pins and the CFRP. Thereafter the titanium pins, in contrast to the stainless steel pins, were not able to maintain the joint's stiffness.

One method to account for this loss in stiffness in the S-N curves is to define failure by a specific decrease in dynamic stiffness. Thus, in this study an arbitrary value of 10 percent loss in dynamic stiffness was chosen as the failure criterion instead of the fatigue strength in Figure 2. Figure 5 shows the resulting S-N curves. When considering 90 % of the original stiffness as a critical value, the exponents k of the S-N curves for both kinds of reinforcement decreased to a value of around 5. Hence both curves are steeper than the fatigue strength based S-N curves. It is assumed, that after failure of the bond line, the pins are solely bearing the loads and thus postponing final failure. A comparison of the strength based S-N curves to the stiffness based S-N curves may hence allow an estimation of the quality of the pin reinforcement. Nevertheless the scatter of the curves $1/T_N$ increased by 180 % in the case of

the stainless steel pin reinforced samples and 60 % for the titanium pin reinforced samples, when applying the stiffness based failure criterion (see values for $1/T_N$ in Figure 2 and Figure 5). This is due to a limitation in frame numbers for the digital image correlation system, which was used for the calculation of the local shear strains. Images were captured every n^{th} cycle and therefore n limits the resolution of the stiffness based approach.

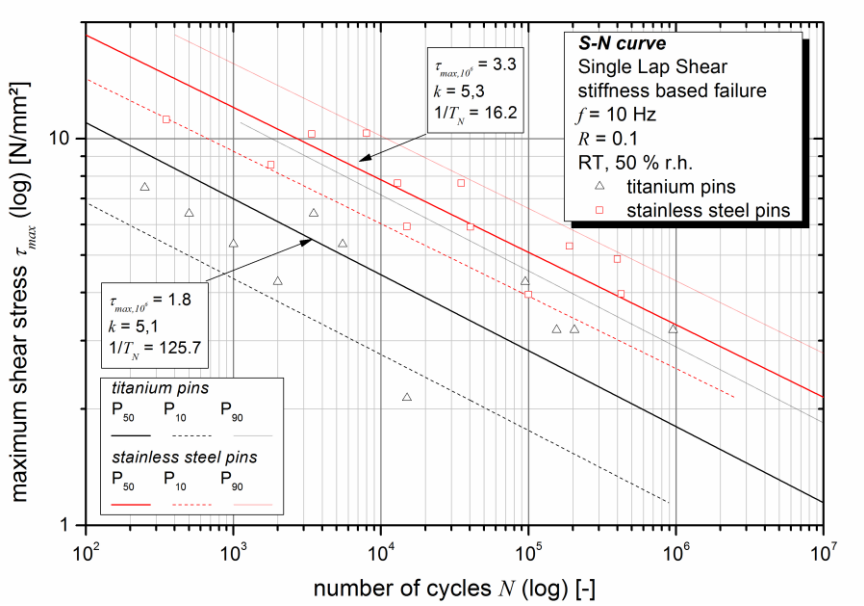

Figure 5. S-N curve for SLS specimens reinforced with CMT welded stainless steel and titanium pins, when considering a 10 % loss in stiffness as failure criterion. P_{10}, P_{50} and P_{90} represent curves for 10, 50 and 90 % propability of survival, respectively. k is the exponent of the S-N curve and $1/T_N$ represents the scatter of the S-N curves between P_{10} and P_{90}.

4. Conclusion and outlook

Cold metal transfer welded pins proved to be an effective means for reinforcing adhesive-bonded or co-cured CFRP-CFRP SLS joints in the through thickness direction. After failure of the bond line between the two CFRP laps, pins carried the loads until final failure. Measurements of the strain distributions on the surface of the specimens via digital image correlation turned out to be a powerful tool for assessing the failure behavior. It gave information about damage initiation, interface failure and subsequent damage mechanisms related to the pin reinforcement. Stainless steel pin inserts turned out to be more effective for reinforcing CFRP laps than titanium pin inserts. This can be partly ascribed to the lack of a pronounced ballhead-spike geometry in the case of titanium pins. Welding process improvements for titanium may be reached by the use of a laser in the welding process.

Apart from the fatigue strength based S-N approach, a stiffness based S-N approach was used to assess the quality of the joint. Together with digital image correlation this approach turned out to be an effective means to evaluate the joint's quality and the reinforcement effect of the different metal inserts.

Acknowledgement

The funding of the Austrian Research Promotion Agency for project 830384 "Composite+composite Joints with Enhanced damage toleranCe (CoJEC)" is gratefully acknowledged as well as the support of the involved project partners FACC AG, Fronius International GmbH, Rübig GmbH & Co KG, Fill GmbH, RECENDT GmbH, Austrian Institute of Technology GmbH and Airbus Group. Installation of the welding robot by Martin Schickbauer at Fill GmbH, specimen production by Gerhard Sieglhuber from Fill GmbH, calibration of the welding machine by Andreas Waldhoer from FRONIUS International GmbH and support in testing by Jürgen Grosser at the Montanuniversität Leoben are gratefully acknowledged.

References

[1] Mouritz AP. Fracture and tensile fatigue properties of stitched fibreglass composites, *Proc. Instn. Mech. Engrs., 218*, 87–93, 2003.

[2] Cartié DD, Laffaille J, Partridge IK, Brunner AJ. Fatigue delamination behaviour of unidirectional carbon fibre/epoxy laminates reinforced by Z-Fiber® pinning, *Engineering Fracture Mechanics,* 76(18): 2834–45, 2009.

[3] Aymerich F. Experimental investigation into the effect of edge stitching on the tensile strength and fatigue life of co-cured joints between cross-ply adherends. *Advanced Composites Letters*, 13(3):151–61, 2004.

[4] Ji H, Kweon J, Choi J. Fatigue characteristics of stainless steel pin-reinforced composite hat joints, *Composite Structures,* 108:49–56, 2014.

[5] Son H, Park Y, Kweon J, Choi J. Fatigue behaviour of metal pin-reinforced composite single-lap joints in a hygrothermal environment, *Composite Structures,* 108:151–60, 2014.

[6] Marasco AI, Cartié DD, Partridge IK, Rezai A. Mechanical properties balance in novel Z-pinned sandwich panels: Out-of-plane properties, *Composites Part A: Applied Science and Manufacturing,* 37(2):295–302, 2006.

[7] Cartié D, Cox B, Fleck NA. Mechanisms of crack bridging by composite and metallic rods, *Composites Part A: Applied Science and Manufacturing*, 35(11):1325–36, 2004.

[8] Dell'Anno G, Cartié DD, Partridge IK, Rezai A. Exploring mechanical property balance in tufted carbon fabric/epoxy composites, *Composites Part A: Applied Science and Manufacturing,* 38(11):2366–73, 2007.

[9] Cartié DD, Dell'Anno G, Poulin E, Partridge IK. 3D reinforcement of stiffener-to-skin T-joints by Z-pinning and tufting, *Engineering Fracture Mechanics,* 73(16):2532–40, 2006.

[10] Löbel T, Kolesnikov B, Scheffler S, Stahl A, Hühne C. Enhanced tensile strength of composite joints by using staple-like pins: Working principles and experimental validation, *Composite Structures,* 106:453–60, 2013.

[11] Graham D, Rezai A, Baker D, Smith PA, Watts JF. A hybrid joining scheme for high strength multi-material joints. In *Proceedings of the 18th International Conference on Composite Materials*. Jeju; South Corea; 2011.

[12] Cartié DD, Troulis M, Partridge IK. Delamination of Z-pinned carbon fibre reinforced laminates, *Composites Science and Technology,* 66(6):855–61, 2006.

[13] Partridge IK, Cartié DD. Delamination resistant laminates by Z-Fiber® pinning: Part I manufacture and fracture performance, *Composites Part A: Applied Science and Manufacturing*, 36(1):55–64, 2005.

[14] Aymerich F, Priolo P, Sun C. Static and fatigue behaviour of stitched graphite/epoxy composite laminates, *Composites Science and Technology,* 63(6):907–17, 2003.

[15] Mouritz A, Leong K, Herszberg I. A review of the effect of stitching on the in-plane mechanical properties of fibre-reinforced polymer composites, *Composites Part A: Applied Science and Manufacturing,* 28:979–91, 1997.

[16] Chang P, Mouritz A, Cox B. Properties and failure mechanisms of pinned composite lap joints in monotonic and cyclic tension, *Composites Science and Technology,* 66(13):2163–76, 2006.

[17] Abdel Wahab M, Ashcroft I, Crocombe A, Smith P. Finite element prediction of fatigue crack propagation lifetime in composite bonded joints, *Composites Part A: Applied Science and Manufacturing,* 35(2):213–22, 2004.

[18] Ishii K, Imanaka M, Nakayama H, Kodama H. Evaluation of the fatigue strength of adhesively bonded CFRP/metal single and single-step double-lap joints, *Composites Science and Technology,* 59(11):1675–83, 1999.

[19] Krenk S, Jönsson J, Hansen L. Fatigue analysis and testing of adhesive joints, *Engineering Fracture Mechanics,* 53(6):859–72, 1996.

[20] Shah Khan MZ, Mouritz AP. Fatigue behaviour of stitched GRP laminates. *Composites Science and Technology,* 56:695–701, 1996.

[21] Schierl A. The CMT process, a revolution in welding technology, *Welding in the world,* 49:38, 2005.

[22] Korya C, Sanderson T. Method of forming a joint (US patent 2011/0240200 A1); 2011.

[23] Stelzer S, Ucsnik S, Tauchner J, Unger T, Pinter G. Novel composite-composite joining technology with through the thickness reinforcement for enhanced damage tolerance. In *Proceedings of the 19th International Conference on Composite Materials*, 4645–4653, 2013.